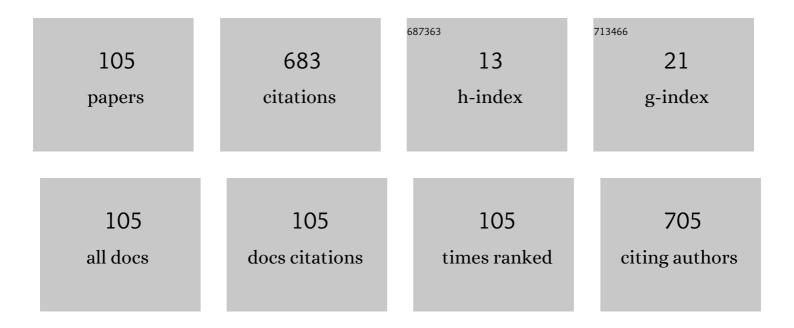
## Hyuongho Ko

List of Publications by Year in descending order

Source: https://exaly.com/author-pdf/166546/publications.pdf Version: 2024-02-01



Нуцомено Ко

#	Article	IF	CITATIONS
1	Low-Noise Resistive Bridge Sensor Analog Front-End Using Chopper-Stabilized Multipath Current Feedback Instrumentation Amplifier and Automatic Offset Cancellation Loop. IEEE Access, 2022, 10, 12385-12394.	4.2	9
2	Low-noise delta-sigma analog front end with capacitor swapping technique for capacitive microsensors. Measurement and Control, 2022, 55, 239-246.	1.8	1
3	Implementation of Flip-Chip Microbump Bonding between InP and SiC Substrates for Millimeter-Wave Applications. Micromachines, 2022, 13, 1072.	2.9	1
4	Current-Reused Current Feedback Instrumentation Amplifier for Low Power Leadless Pacemakers. IEEE Access, 2021, 9, 113748-113758.	4.2	3
5	A Four-Channel Low-Noise Readout IC for Air Flow Measurement Using Hot Wire Anemometer in 0.18 μm CMOS Technology. Sensors, 2021, 21, 4694.	3.8	4
6	Low-Noise Chopper Amplifier Using Lateral PNP Input Stage With Automatic Base Current Cancellation. IEEE Transactions on Circuits and Systems II: Express Briefs, 2021, 68, 2297-2301.	3.0	4
7	Artificial Compound Eye Systems and Their Application: A Review. Micromachines, 2021, 12, 847.	2.9	19
8	Compact Weather Sensor Node for Predicting Road Surface Temperature. Sensors and Materials, 2021, 33, 2763.	0.5	2
9	Chopper-stabilized Multipath Instrumentation Amplifier with Output Voltage Offset Compensation Using R-2R Digital-to-Analog Converter. Sensors and Materials, 2021, 33, 2709.	0.5	0
10	A Low-Power, Low-Noise, Resistive-Bridge Microsensor Readout Circuit with Chopper-Stabilized Recycling Folded Cascode Instrumentation Amplifier. Applied Sciences (Switzerland), 2021, 11, 7982.	2.5	8
11	A Potentiostat Readout Circuit with a Low-Noise and Mismatch-Tolerant Current Mirror Using Chopper Stabilization and Dynamic Element Matching for Electrochemical Sensors. Applied Sciences (Switzerland), 2021, 11, 8287.	2.5	4
12	Phase Locked Loop based Resonator Driving IC with Negative Charge Cancelling. , 2020, , .		0
13	A 5.43 nV/â^šHz Chopper Operational Amplifier Using Lateral PNP Input Stage with BJT Current Mirror Base Current Cancellation. Applied Sciences (Switzerland), 2020, 10, 8376.	2.5	1
14	Power Line Interference Reduction Technique with a Current-Reused Current-Feedback Instrumentation Amplifier for ECG Recording. Applied Sciences (Switzerland), 2020, 10, 8478.	2.5	4
15	Low-Noise Chopper-Stabilized Multi-Path Operational Amplifier with Nested Miller Compensation for High-Precision Sensors. Applied Sciences (Switzerland), 2020, 10, 281.	2.5	7
16	Chopper-Stabilized Low-Noise Multipath Operational Amplifier With Dual Ripple Rejection Loops. IEEE Transactions on Circuits and Systems II: Express Briefs, 2020, 67, 2427-2431.	3.0	8
17	Fully Differential Chopper-Stabilized Multipath Current-Feedback Instrumentation Amplifier with R-2R DAC Offset Adjustment for Resistive Bridge Sensors. Applied Sciences (Switzerland), 2020, 10, 63.	2.5	17
18	Low-Noise Multimodal Reconfigurable Sensor Readout Circuit for Voltage/Current/Resistive/Capacitive Microsensors. Applied Sciences (Switzerland), 2020, 10, 348.	2.5	6

#	Article	IF	CITATIONS
19	A 24.88 nV/â^šHz Wheatstone Bridge Readout Integrated Circuit with Chopper-Stabilized Multipath Operational Amplifier. Applied Sciences (Switzerland), 2020, 10, 399.	2.5	9
20	Open-loop Spectrum Analyzer Integrated Circuit for Nanoresonator Sensing. Sensors and Materials, 2020, 32, 2215.	0.5	1
21	Self-Biased Ultralow Power Current-Reused Neural Amplifier With On-Chip Analog Spike Detections. IEEE Access, 2019, 7, 109792-109803.	4.2	9
22	A New Simple Fabrication Method for Silicon Nanowire-Based Accelerometers. , 2019, , .		5
23	Twelve-day medium pumping into tubular cell-laden scaffold using a lab-made PDMS connector. , 2019, 38, 1-13.		5
24	A low-power 33 pJ/conversion-step 12-bit SAR resistance-to-digital converter for microsensors. Microsystem Technologies, 2019, 25, 2093-2098.	2.0	4
25	164ÂnW Inverter-based capacitive readout IC for microaccelerometer. Microsystem Technologies, 2019, 25, 2035-2040.	2.0	4
26	Low-phase-noise self-sustaining amplifier IC with parallel capacitance cancellation for low-Q piezoelectric resonator. Microsystem Technologies, 2019, 25, 2041-2050.	2.0	3
27	Low-noise 16-bit First-order Delta-sigma Capacitance-to-digital Converter for Capacitive Humidity Sensor. Sensors and Materials, 2019, 31, 1523.	0.5	1
28	Low-noise Analog Front-end with Chopper-stabilized Multipath Current-feedback Instrumentation Amplifier for Resistive Sensors. Sensors and Materials, 2019, 31, 1697.	0.5	2
29	Secure Circuit with Low-power On-chip Temperature Sensor for Detection of Temperature Fault Injection Attacks. Sensors and Materials, 2019, 31, 1375.	0.5	0
30	4.36 fJ/Conversion-step Ultralow-power 16-bit Successive Approximation Register Capacitance-to-digital Converter in 0.18 ��m CMOS Process. Sensors and Materials, 2019, 31, 1535.	0.5	0
31	Secure Integrated Circuit with Physical Attack Detection based on Reconfigurable Top Metal Shield. Journal of Semiconductor Technology and Science, 2019, 19, 260-269.	0.4	0
32	Biosignal integrated circuit with simultaneous acquisition of ECG and PPG for wearable healthcare applications. Technology and Health Care, 2018, 26, 3-9.	1.2	5
33	Characterization of the Piezoresistive Effects of Silicon Nanowires. Sensors, 2018, 18, 3304.	3.8	7
34	Nanowire-Based Biosensors: From Growth to Applications. Micromachines, 2018, 9, 679.	2.9	99
35	Increased piezoresistive effects of silicon nanowires for effective biomimetic sensing. , 2018, , .		1
36	Reconfigurable Sensor Analog Front-End Using Low-Noise Chopper-Stabilized Delta-Sigma Capacitance-to-Digital Converter. Micromachines, 2018, 9, 347.	2.9	8

#	Article	IF	CITATIONS
37	0.6 V, 116 nW Neural Spike Acquisition IC with Self-Biased Instrumentation Amplifier and Analog Spike Extraction. Sensors, 2018, 18, 2460.	3.8	9
38	Secure circuit with optical energy harvesting against unpowered physical attacks. Computers and Electrical Engineering, 2018, 70, 74-82.	4.8	0
39	Low-noise Reconfigurable 12- to 16-bit Delta-Sigma Capacitance-to-digital Converter with Chopper Stabilization Technique. Sensors and Materials, 2018, 30, 1671.	0.5	1
40	31.6 pJ/Conversion-step Energy-efficient 16-bit Successive Approximation Register Capacitance-to-digital Converter in a 0.18 μm CMOS Process. Sensors and Materials, 2018, 30, 1765.	0.5	1
41	Review of High-resolution Retinal Prosthetic System for Vision Rehabilitation: Our Perspective Based on 18 Years of Research. Sensors and Materials, 2018, 30, 1393.	0.5	4
42	The lunar terrain imager operations concepts. , 2018, , .		2
43	Capacitive analog front-end circuit with dual-mode automatic parasitic cancellation loop. Microsystem Technologies, 2017, 23, 515-523.	2.0	6
44	Electrical characterization of 2D and 3D microelectrodes for achieving high-resolution sensing in retinal prostheses with in vitro animal experimental results. Microsystem Technologies, 2017, 23, 473-481.	2.0	7
45	Fabrication of a MEMS retinal tack and long-term in vivo biocompatibility evaluation for retinal prostheses. Microsystem Technologies, 2017, 23, 483-489.	2.0	1
46	Low Noise and Low Power IC Using Opamp Sharing Technique for Capacitive Micro-Sensor Sensing Platform. Journal of Sensor Science and Technology, 2017, 26, 60-65.	0.2	0
47	Low-Power Photoplethysmogram Acquisition Integrated Circuit with Robust Light Interference Compensation. Sensors, 2016, 16, 46.	3.8	23
48	A Dynamic Instrumentation Amplifier for Low-Power and Low-Noise Biopotential Acquisition. Sensors, 2016, 16, 354.	3.8	6
49	Reconfigurable Multiparameter Biosignal Acquisition SoC for Low Power Wearable Platform. Sensors, 2016, 16, 2002.	3.8	14
50	A 1.2 V Low-Power CMOS Chopper-Stabilized Analog Front-End IC for Glucose Monitoring. IEEE Sensors Journal, 2016, 16, 6517-6518.	4.7	12
51	Low-Power and Low-Noise Capacitive Sensing IC Using Opamp Sharing Technique. IEEE Sensors Journal, 2016, 16, 7839-7840.	4.7	8
52	Ultralow-Power Bioimpedance IC With Intermediate Frequency Shifting Chopper. IEEE Transactions on Circuits and Systems II: Express Briefs, 2016, 63, 259-263.	3.0	37
53	Electro-Thermal Modeling and Experimental Validation of Integrated Microbolometer with ROIC. Journal of Semiconductor Technology and Science, 2016, 16, 367-374.	0.4	0
54	Biomimetic Gyroscope Integrated with Actuation Parts of a Robot Inspired by Insect Halteres. Journal of Institute of Control, Robotics and Systems, 2016, 22, 705-709.	0.2	0

#	Article	IF	CITATIONS
55	2048-Point Fast Fourier Transform Processing Based on Twiddle Factor Reduction and Dynamic Data Scaling. Advanced Science Letters, 2016, 22, 3662-3666.	0.2	0
56	Chopper stabilized analog front-end IC with improved ripple reduction loop. , 2015, , .		0
57	A Neural Stimulator with Silicon Nanowire Photodetector for Artificial Retinal Prostheses. Journal of Computational and Theoretical Nanoscience, 2015, 12, 769-773.	0.4	3
58	The Anti-Reflection Coating Using the Silicon Nitride and Silicon Monoxide for InP Based Solar Cells. Journal of Computational and Theoretical Nanoscience, 2015, 12, 871-874.	0.4	2
59	Behavioral modeling and experimental validation of uncooled microbolometer. , 2015, , .		1
60	Fully Integrated Low-Noise Readout Circuit with Automatic Offset Cancellation Loop for Capacitive Microsensors. Sensors, 2015, 15, 26009-26017.	3.8	16
61	Analog front-end measuring biopotential signal with effective offset rejection loop. Bio-Medical Materials and Engineering, 2015, 26, S935-S941.	0.6	2
62	Fully Integrated Biopotential Acquisition Analog Front-End IC. Sensors, 2015, 15, 25139-25156.	3.8	23
63	Low noise resistive analog front-end with automatic offset calibration loop. , 2015, , .		1
64	Ambient light cancellation in photoplethysmogram application using alternating sampling and charge redistribution technique. , 2015, 2015, 6441-4.		6
65	Triple cascode high output impedance current stimulator with dynamic element matching for retinal prostheses. , 2015, , .		1
66	Light-Controlled Biphasic Current Stimulator IC Using CMOS Image Sensors for High-Resolution Retinal Prosthesis and <italic>In Vitro</italic> Experimental Results With rd1 Mouse. IEEE Transactions on Biomedical Engineering, 2015, 62, 70-79.	4.2	20
67	Bioinspired Piezoresistive Acceleration Sensor Using Artificial Filiform Sensillum Structure. Sensors and Materials, 2015, , .	0.5	1
68	A Review of Nanotechnology for Highly Sensitive Photodetectors for Vision Sensors of Insect-like Robots. Sensors and Materials, 2015, , .	0.5	2
69	Biomimetic Multiaperture Imaging Systems: A Review. Sensors and Materials, 2015, , .	0.5	2
70	Pulse count modulation based biphasic current stimulator for retinal prosthesis and in vitro experiment using rd1 mouse. , 2014, 2014, 1711-4.		1
71	A fully integrated electroencephalogram (EEG) analog front-end IC with capacitive input impedance boosting loop. , 2014, , .		9
72	A versatile biopotential acquisition analog front end IC with effective DC offset and ripple rejection. , 2014, , .		2

#	Article	IF	CITATIONS
73	High-uniformity post-CMOS uncooled microbolometer focal plane array integrated with active matrix circuit. Sensors and Actuators A: Physical, 2014, 211, 138-144.	4.1	2
74	Integrated current-mode DC–DC boost converter with high-performance control circuit. Analog Integrated Circuits and Signal Processing, 2014, 80, 105-112.	1.4	8
75	Capacitive Readout Circuit for Tri-axes Microaccelerometer with Sub-fF Offset Calibration. Journal of Semiconductor Technology and Science, 2014, 14, 83-91.	0.4	8
76	A 16-channel Neural Stimulator IC with DAC Sharing Scheme for Artificial Retinal Prostheses. Journal of Semiconductor Technology and Science, 2014, 14, 658-665.	0.4	2
77	The Micro Pirani Gauge with Low Noise CDS-CTIA for In-Situ Vacuum Monitoring. Journal of Semiconductor Technology and Science, 2014, 14, 733-740.	0.4	3
78	An analog front-end IC with regulated R-I amplifier and CDS CTIA for microbolometer. , 2013, , .		5
79	A 16-channel neural stimulator with DAC sharing scheme for visual prostheses. , 2013, , .		1
80	High-uniformity post-CMOS uncooled microbolometer focal plane array integrated with active matrix circuit. , 2013, , .		0
81	Area-efficient RC low pass filter using T-networked resistors and capacitance multiplier. , 2013, , .		7
82	Current Stimulator IC with Adaptive Supply Regulator for Visual Prostheses. Journal of Biomedical Nanotechnology, 2013, 9, 992-997.	1.1	1
83	Multi-Channel Stimulator IC Using a Channel Sharing Method for Retinal Prostheses. Journal of Biomedical Nanotechnology, 2013, 9, 621-625.	1.1	8
84	An Arbitrary Waveform 16 Channel Neural Stimulator with Adaptive Supply Regulator in 0.35 ㎛ HV CMOS for Visual Prosthesis. Journal of Semiconductor Technology and Science, 2013, 13, 79-86.	0.4	0
85	Sub-fF trimmable readout circuit for tri-axes capacitive microaccelerometers. , 2012, , .		5
86	Highly configurable capacitive interface circuit for triâ€axial MEMS microaccelerometer. International Journal of Electronics, 2012, 99, 945-955.	1.4	5
87	Low noise accelerometer microsystem with highly configurable capacitive interface. Analog Integrated Circuits and Signal Processing, 2011, 67, 365-373.	1.4	6
88	Highly programmable temperature compensated readout circuit for capacitive microaccelerometer. Sensors and Actuators A: Physical, 2010, 158, 72-83.	4.1	31
89	Optimal and Robust Design Method for Two-Chip Out-of-Plane Microaccelerometers. Sensors, 2010, 10, 10524-10544.	3.8	7
90	Non-ideal behavior of a driving resonator loop in a vibratory capacitive microgyroscope. Microelectronics Journal, 2008, 39, 1-6.	2.0	11

#	Article	IF	CITATIONS
91	Multi-channel capacitive readout IC for MEMS inertial sensors. , 2008, , .		0
92	A 16-bit ultra-thin tri-axes capacitive microaccelerometer for mobile application. , 2007, , .		2
93	A 37 ppm/l̂¼C Temperature Compensated CMOS ASIC with $\hat{A}\pm 16$ V Supply Protection for Capacitive Microaccelerometers. , 2007, , .		0
94	Wafer-level hermetic packaged microaccelerometer with fully differential BiCMOS interface circuit. Sensors and Actuators A: Physical, 2007, 137, 25-33.	4.1	11
95	High Performance Microaccelerometer with Wafer-level Hermetic Packaged Sensing Element and Continuous-time BiCMOS Interface Circuit. Journal of Physics: Conference Series, 2006, 34, 1002-1007.	0.4	1
96	Modeling and Simulation of the Microgyroscope Driving Loop using SPICE. Journal of Physics: Conference Series, 2006, 34, 1020-1025.	0.4	2
97	Wafer-level Hermetic Packaged Dual-axis Digital Microaccelerometer. , 2006, , .		1
98	Selective silicon-on-insulator (SOI) implant: a new micromachining method without footing and residual stress. Journal of Micromechanics and Microengineering, 2005, 15, 1607-1613.	2.6	16
99	An x-axis single-crystalline silicon microgyroscope fabricated by the extended SBM process. Journal of Microelectromechanical Systems, 2005, 14, 444-455.	2.5	18
100	Robust SOI process without footing and its application to ultra high-performance microgyroscopes. Sensors and Actuators A: Physical, 2004, 114, 236-243.	4.1	21
101	A NOVEL Z-AXIS ACCELEROMETER WITH PERFECTLY-ALIGNED, FULLY-OFFSET VERTICAL COMBS FABRICATED USING THE EXTENDED SACRIFICIAL BULK MICROMACHINING PROCESS. International Journal of Computational Engineering Science, 2003, 04, 493-496.	0.1	3
102	A new isolation method for single crystal silicon MEMS and its application to z-axis microgyroscope. , 0, , .		6
103	Two-chip implemented, wafer-level hermetic packaged accelerometer for tactical and inertial applications. , 0, , .		1
104	The first sub-deg/HR bias stability, silicon-microfabricated gyroscope. , 0, , .		6
105	PLL-based nanoresonator driving IC with automatic parasitic capacitance cancellation and automatic gain control. Measurement and Control, 0, , 002029402110293.	1.8	1